



## Study on microstructures and properties of carbide-free and carbide-bearing bainitic steels



Xiaoyan Long<sup>a</sup>, Fucheng Zhang<sup>a,b,\*</sup>, Zhinan Yang<sup>b</sup>, Bo Lv<sup>c</sup>

<sup>a</sup> State Key Laboratory of Metastable Materials Science and Technology, Yanshan University, Qinhuangdao 066004, China

<sup>b</sup> National Engineering Research Center for Equipment and Technology of Cold Strip Rolling, Yanshan University, Qinhuangdao 066004, China

<sup>c</sup> College of Environmental and Chemical Engineering, Yanshan University, Qinhuangdao 066004, China

### ARTICLE INFO

#### Keywords:

Bainite  
Carbide  
Microstructure  
Property

### ABSTRACT

The microstructural characteristics, the mechanical and fatigue properties of carbide-free lower bainite and carbide-bearing lower bainite were studied. Moreover, the effects of the bainitic ferrite, retained austenite, and carbide phases on the properties of the tested steels were analyzed. Results show that the carbide-free lower bainite consists of fine bainitic ferrite plates and metastable retained austenite. Large amounts of C atoms are distributed in the metastable retained austenite. The carbide-bearing lower bainite consists of thick bainitic ferrite plates and stable carbides, which contain numerous C atoms. Carbide-free lower bainite exhibits higher strength, plasticity, and toughness than carbide-bearing lower bainite, and the former also exhibits longer fatigue life under total strain amplitude, the latter exhibits longer fatigue life under plastic strain amplitude. The metastable retained austenite of large size in the carbide-free lower bainite obviously undergoes strain-induced martensitic transformation during deformation. Martensitic transformation delays crack propagation by absorbing the energy required for crack propagation, thus increasing the fatigue life of carbide-free lower bainite under total strain amplitude. The stable carbide and the coarse bainite ferrite plates play positive roles for the fatigue life under plastic strain amplitude, while the fine bainite ferrite plates and metastable retained austenite are negative. The stable secondary carbide phase strengthens carbide-bearing lower bainite under uniaxial tensile deformation but may shorten fatigue life under cyclic fatigue by acting as locations of stress concentration.

### 1. Introduction

The various morphologies of the bainite microstructure in bainitic steels have attracted considerable research attention. Bainitic steel has been designed and manufactured in bearing, gear, railway (including rails and crossings) and other industries [1–5]. Bainite rails and crossings, made of low/medium carbon and low alloying steels, have received wide attention and recognition because of their good service performance. With the development trend of railways towards heavy-load and high-speed, there is an urgent need to further improve the comprehensive performance of the bainite rails and crossings [5,6]. Bainite morphology is closely related to the elements of the alloying components. Carbide-free bainite is generally fabricated using steel alloyed with silicon (Si) and/or aluminum (Al). The transformation of Si and Al is retarded by their extremely low solubility in cementite [7–9]. Therefore, the chemical composition design of bainite steels used for railway systems offer great theoretical research and practical engineering significances.

These engineering parts are exposed to dynamic cyclic loading. Therefore, the cyclic deformation mechanism of bainitic steels during low-cycle fatigue is worth investigating. Hilditch et al. found that the manner through which different microstructural phases accommodate applied cyclic strain could influence the strain life and cyclic-stabilized strength of the bainitic steel [10]. Lucas and Gerberich [11] found that the initial dislocation density of martensitic/austenitic steel with acicular ferrite or bainite microstructures decreases during strain hardening under fatigue and the ferrite grain boundaries and M/A island decrease crack propagation rate [12]. Sankaran et al. [13,14] found that austenite films retained between bainitic ferrite plates prevent the softening of high-strength ferritic/bainitic/martensitic steel during low-cycle fatigue. Branco et al. [15] reported that the low-cycle fatigue behavior of high-strength steel with martensitic and lower bainitic microstructures is affected by microstructural defects. Rementeria et al. reported that high amounts of stable retained austenite in carbide-free bainitic steel alloyed with high carbon content increase the numbers of nucleation sites for fatigue cracks and possibly increase stress

\* Corresponding author at: State Key Laboratory of Metastable Materials Science and Technology, Yanshan University, Qinhuangdao 066004, China.  
E-mail address: [zfc@ysu.edu.cn](mailto:zfc@ysu.edu.cn) (F. Zhang).

concentration at ferrite–austenite interphases [16]. Yang showed that film-like retained austenite and secondary cracks positively affect the high-cycle bending fatigue behavior of low-temperature bainitic steel [17]. Yu studied carbide-free bainite/martensite steel and found that sample surface, inclusions and defects, and soft or coarsely soft structures all influence fatigue behavior [18]. Georgiyev showed that among different structural states with the same strength in medium-carbon steel, the carbide-free bainite microstructure possesses the highest cyclical crack resistance, which results from the stable retained austenite microstructure [19]. These studies focused on the comparison of carbide-free bainite with martensitic steel and ferritic steels, but few works have conducted a comparative study of carbide-bearing bainite and carbide-free bainite microstructures.

A three-dimensional atomic probe could be used to effectively detect the elemental segregation and composition of austenitic, bainitic, and martensitic microstructures [20–23]. Bhadeshia and Caballero explored the distribution of carbon and alloying elements in the bainitic ferrite phase and the retained austenite phase in bainitic steels by using atom probe tomography (APT), X-ray diffraction (XRD) measurements, and transmission electron microscopy (TEM) [24–29]. The researchers investigated carbon supersaturation in bainitic ferrite in low-temperature bainite and found that supersaturated carbon is mainly trapped in the Cottrell atmosphere and the bainite ferrite lattice. In a previous study, we did not observe the redistribution of substitutional atoms between bainitic ferrite and retained austenite/martensite before and after cyclic deformation [30]. In this study, the distribution of carbon atoms and its effects on properties of bainitic steels through APT were investigated.

Two kinds of bainitic steels were designed in the present study. One kind of steel was alloyed with Si and Al to introduce carbide-free bainite, whereas the other kind of steel was not alloyed with Si and Al to introduce carbide-bearing bainite. The microstructures, mechanical properties, and fatigue behaviors of the fabricated bainitic steels were studied. Moreover, the effects of bainitic ferrite, retained austenite, and carbide phases on the properties of the bainitic steels were analyzed.

## 2. Experimental material and procedures

The chemical compositions of the tested steels used in this study are shown in Table 1. The contents of C, Mn, Cr, Mo, and Ni are virtually identical. 1.48Si + 0.71Al were added to one steel but not to the other. The tested steels were synthesized using vacuum smelting and forging, and the forging ratio is about 6. The contents of S, P and N are all below 0.01%, as shown in the Table 1. The effect of these elements with such low content on steel performance could be neglected.

The Ms temperatures were measured by a DIL805A thermodilatometry. Each sample was machined into a cylinder with a diameter of 4 mm and height of 10 mm. Samples were heated at a rate of  $10\text{ }^{\circ}\text{C s}^{-1}$  to austenitisation temperature ( $930\text{ }^{\circ}\text{C}$ ) and held for 10 min. Subsequently, samples were cooled to room temperature at a rate of  $30\text{ }^{\circ}\text{C s}^{-1}$ . The test curves and Ms temperatures was shown in Fig. 1 and Table 1, respectively.

All samples were austenitized at  $930\text{ }^{\circ}\text{C}$ . To obtain steels with lower bainite, the steels underwent isothermal heat treatment at  $M_s + 10\text{ }^{\circ}\text{C}$  after austenitization and holding for 1 h. The isothermal temperature is chosen to obtain finer microstructure in the tested steels.

**Table 1**  
Chemical composition of tested bainitic steels.

		C	Si	Mn	Cr	Ni	Mo	Al	S	P	N	Ms, $^{\circ}\text{C}$
Carbide-free-B	wt%	0.34	1.48	1.52	1.15	0.93	0.40	0.71	0.003	0.006	0.002	310
	at%	1.51	2.82	1.48	1.18	0.85	0.22	1.41				
Carbide-bearing-B	wt%	0.34	0.01	1.61	1.24	0.96	0.45	0.04	0.002	0.005	0.003	340
	at%	1.56	0.04	1.62	1.32	0.90	0.26	0.08				

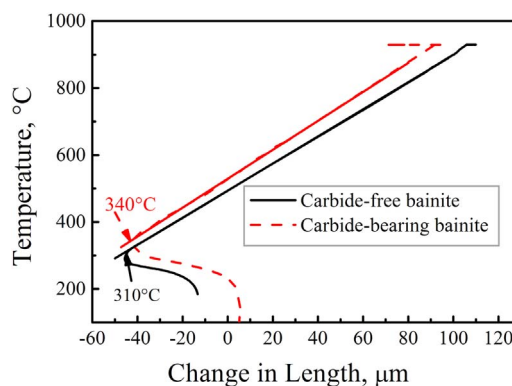


**Fig. 1.** Ms temperature tested curves.

The tensile test was conducted using a MTS material testing machine with a crosshead speed of 0.3 mm/min. Tensile samples with a gauge of 25 mm and a gauge diameter of 5 mm were fabricated and three samples were tested for each process. Impact toughness was measured at  $+20\text{ }^{\circ}\text{C}$  using a 300 J Charpy testing machine with a U-notch 2 mm in width and the sample size of  $10\text{ mm} \times 10\text{ mm} \times 55\text{ mm}$ . A TH501 Digital Rockwell hardness tester was used to determine the hardness of the samples.

Low-cycle fatigue (LCF) testing was performed with an MTS Servo-Hydraulic Test System (Landmark 100 kN with 370.10 Load Frame). Samples with a gauge length of 10 mm and gauge diameter of 5 mm were machined. The tests were controlled with total strain amplitudes of 0.6%, 0.7%, 0.8%, and 1.0%. A sinusoidal waveform ( $R = -1$ ) at a constant strain rate of  $6 \times 10^{-3}\text{ s}^{-1}$  was used.

Microstructures were characterized and analyzed using an SU-5000 type thermal-emission scanning electron microscopy (SEM). The microstructures were examined using a Hitachi H-800 transmission electron microscope operated at 200 kV. The samples were thinned to perforation on a TenuPol-5 twinjet unit with an electrolyte consisting of 7% perchloric and 93% glacial acetic acids. The voltage and temperature for electropolishing were approximately 29 V and  $25\text{ }^{\circ}\text{C}$ , respectively. The partition of the alloying atoms in the microstructures was analyzed using APT. Samples were cut using a wire electrical discharge machining to obtain thin rods of  $0.5\text{ mm} \times 0.5\text{ mm} \times 15\text{ mm}$ . The surfaces were then polished using sandpapers followed by chemical polishing [31]. First, 75% acetic acid and 25% perchloric acid were used to induce corrosion, and ethylene glycol monobutyl ether solution ( $\text{C}_6\text{H}_{14}\text{O}_2$ ) with 2% high chlorine acid was applied to further induce corrosion. Finally, the blunt needles of the experiments were obtained. Finally, the required blunt needles for the experiments were obtained. The tip samples were analyzed on an Imago Scientific Instrument LEAP 3000 h through a local electrode method. The samples were cooled to 50 K with a pulse frequency of 5 kHz and 20% pulse fraction. To reconstruct the three-dimensional spatial distribution of carbon atoms, the collected data were processed and analyzed using IVAS software (integrated visualization and analysis software).

Download English Version:

<https://daneshyari.com/en/article/7973542>

Download Persian Version:

<https://daneshyari.com/article/7973542>

[Daneshyari.com](https://daneshyari.com)